Journal of ELECTRICAL ENGINEERING, VOL 69 (2018), NO6, 431–434

sciendo

COMMUNICATIONS

Magnetic measurement of permanent magnet by 40 T long pulse magnet

Masato Enokizono*, Koji Yamada, Yasushi Nakahata*****

Permanent magnets, especially Nd-Fe-B magnets are very important engineering elements that are widely used in many applications. Detailed design of electrical and electronic equipment using permanent magnets requires precise measurement of magnetic characteristics. We developed a measurement system which can measure the magnetic characteristics of permanent magnets precisely. This paper presents the measured results of magnetic characteristics of various types of permanent magnets and comparison of these characteristics.

K e y w o r d s: pulsed high magnetic field, pulse magnetizer, pulse coil, magnetization characteristics

1 Introduction

The permanent magnets with large remanence, larger than 1 T as in Nd-Dy-Fe-B compounds, have been used in industry and will play important role in the future electric vehicles. However, full magnetization of such magnets with high demagnetization constant might be very difficult using conventional magnetizers due to low applied field. Furthermore, the precise observations of $M - H$ curve have not been performed yet. Frequency dispersion of the magnetization caused by the slow domain movements in high and fast fields in the range of several Ts make such measurements difficult. In this study, we show the structure of the pulsed field magnetizer [1-3] with relatively short half width of 10 ms for 40 T field and with a long rise up time of 30 ms for 20 T field. Using this pulsed magnetic field generator, we attained high precision in measurements of $M - H$ curves - within 3% error [4]. We have also found some enhancements of remanence caused by the forced domain reorientation as an effect of application of high magnetic field without the slow decrease in the remanence (so called magnetization after-effect). We show the details of the electric circuitry of our device and the measurement technology [5]. The facility of the large scaled magnetizer was constructed in Oita Prefectural Organization for Industry Creation.

2 Pulse magnetizer system

We designed and assembled a pulsed power supply magnetizer (later called simply the magnetizer) for performing low-frequency pulsed excitation with a high magnetic field. The magnetizer circuit diagram is presented in Fig. 1 and the photograph of it in Fig. 2. The magnetizer power supply was composed of the two large capacitors banks of 28 mF at 3 kV and 100 mF at 1 kV for the purpose of generator of short and long pulses. A large scaled thyristor with the performance index of 2.4×10^7 ($I_{\max}^2 \tau$, where, $I_{\max}$ stands for the maximum current and τt is the half-pulsed width, respectively) serves as a main shot switch. The capacitors are charged via a rectifier. The thyristor is triggered by an optical fiber, which provides electrical isolation for safety. Under normal conditions the current is in dumped oscillation. Under non-oscillatory conditions (with crowbar circuit) the current is unipolar oscillation waveform makes it possible to demagnetize a magnetized sample. The direction of the generated magnetic field can be changed with a polarity selection switch, allowing measurement of the hysteresis curve of the sample.

A relatively high magnetic field can be easily generate in a short pulse, but because of eddy current flowing in the

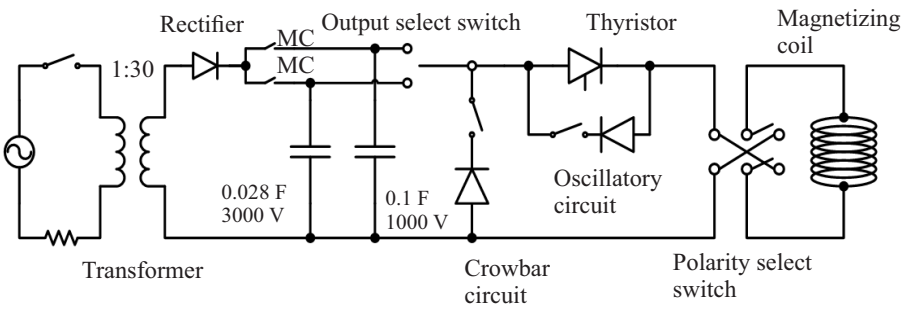

Fig. 1. The structure of the high pulsed magnetic field generator

* Vector Magnetic Characteristic Technical Laboratory, USA, Japan, enoki@oita-u.ac.jp, ** Faculty of Engineering, Saitama University, Saitama, Japan, yamasan@fms.saitama-u.ac.jp, *** Faculty of Engineering, Oita University, Oita, Japan, y.nakahata@oita-mag.jp

DOI: 10.2478/jee-2018–0067, Print (till 2015) ISSN 1335-3632, On-line ISSN 1339-309X

Fig. 2. Photograph of pulse magnetizer

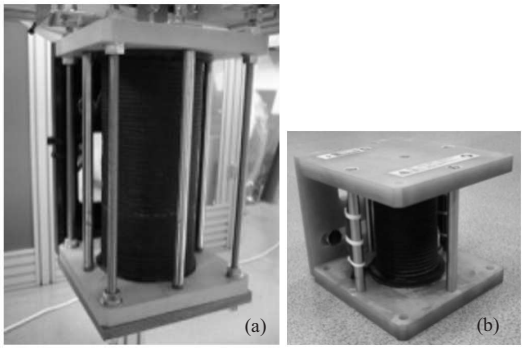

Fig. 3. Photograph of pulse coils:(a)–1500 turns coil,(b)–500 turns coil

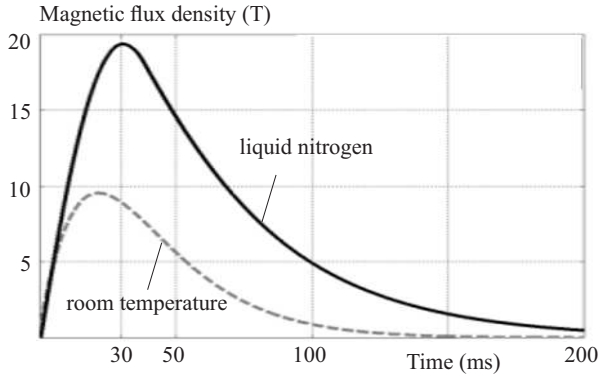

Fig. 4. Influence of magnetizing coils temperature on pulse-field amplitude

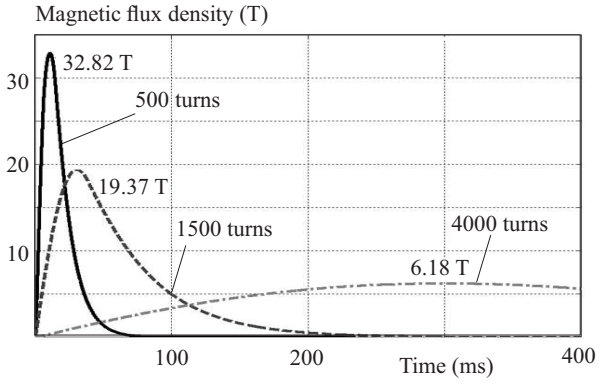

Fig. 5. Influence of magnetizing coils temperature on pulse-field amplitude

magnetized sample, accurate measurement of the magnetization characteristics is not possible. For that reason, it is necessary to generate a long-pulsed magnetic field, which requires a pulsed coil that has a large inductance. Fig. 3 shows the photograph of fabricated pulse coils. The coils were made with soft glass insulated copper wire. The coil was reinforced with the laminated Kevlar fiber. During the measurements the coil was dipped in liquid nitrogen to reduce its resistance down to 15% in comparison to value at RT. A comparison of generated magnetic field showing the effect of the liquid nitrogen cooling is presented in Fig. 4. We see from the figure that the liquid nitrogen cooling increases the generated magnetic field by a factor of two. The experimental field strengths in Fig. 5 are only tentatively shown. The maximum magnetic flux density of the longest curve ($\Delta t = 0.3$ s) might be easily improved as marked 6.18 T was achieved for V_c equal only 800 V for a maximum of 2500 V possible. From the traces of generated fields shown in this figure we can see that the highest field of $B_{max} = 33$ T is possible only with the shortest pulse of 10 ms half width.

3 Magnetization detection coil and search coil

Magnetization detection coils are coming into wide use for measuring the magnetization characteristics of permanent magnets by means of pulsed magnetic fields. When measuring magnetization by the induction method, two coils of opposite directions are connected in series so that no voltage is induced in the detection coil by a changing external magnetic field when no sample is present. The coaxial magnetization detection coil is shown in Fig. 6. The inside coil is for detecting magnetic flux density and the outside coil is the canceling coil.

Here is the measurement principle of the magnetic field strength. We denote the sample cross-sectional area as πr_s^2, the number of turns of Coil-1 as N_1, the cross-sectional area of Coil-1 as πr_1^2, the number of turns of Coil-2 as N_2, and the cross-sectional area of Coil-2 as πr_2^2. The number of turns relation of the coils is $N_1 = N_2$. The respective coil magnetic flux density, magnetic flux, and induced voltage are given by following equations.

$$B_1 = B_2 = \mu_0(H + M) \tag{1}$$

$$\phi_1 = \pi\mu_0\big(r_1^2 H + r_s^2 M\big) \tag{2}$$

$$\phi_2 = \pi\mu_0\big(r_2^2 H + r_s^2 M\big) \tag{3}$$

$$e_1 = -\pi\mu_0 N_1\big(r_1^2\frac{\mathrm{d}H}{\mathrm{d}t} + r_s^2\frac{\mathrm{d}M}{\mathrm{d}t}\big) \tag{4}$$

$$e_2 = -\pi\mu_0 N_2\big(r_2^2\frac{\mathrm{d}H}{\mathrm{d}t} + r_s^2\frac{\mathrm{d}M}{\mathrm{d}t}\big) \tag{5}$$

The difference in induced voltages between Coil-1 and Coil-2 is expressed as the following equation.

$$e_2 - e_1 = -\pi\mu_0\big(N_2 r_2^2 - N_1 r_1^2\big)\frac{\mathrm{d}H}{\mathrm{d}t} \tag{6}$$

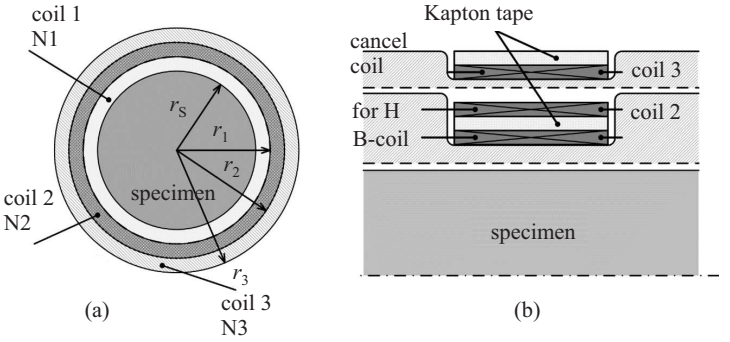

Fig. 6. Structure of coaxial type sensor:(a) – front view of coaxial type sensor, (b) – cross section drawing of coaxial type sensor

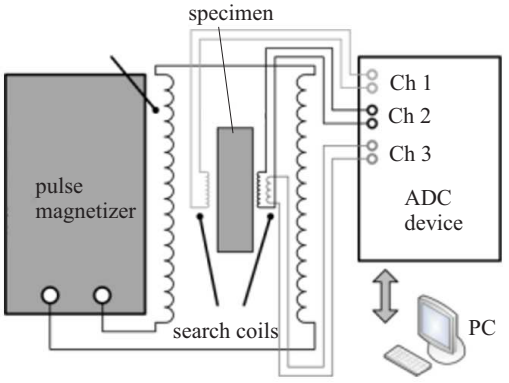

Fig. 7. Block diagram of system for evaluation of permanent magnets in high pulsed fields

The induced voltage includes the time differential of the magnetic field strength H, $\mathrm{d}H/\mathrm{d}t$, so H can be obtained by integrating the induced voltage

$$H(t) = -\frac{\int \big(e_2(t) - e_1(t)\big)\mathrm{d}t}{\mu_0 \pi \big(N_2 r_2^2 - N_1 r_1^2\big)} \tag{7}$$

Here is the measurement principle of the magnetic field. Similarly, we denote the number of turns of Coil-3 as N_3, the cross-sectional area of Coil-3 as πr_2^2. The area turn relation of the coils is $N_1 r_1 = N_3 r_3$. The respective coil magnetic flux density, magnetic flux, and induced voltage are given by following equations

$$B_1 = B_3 = \mu_0 (H + M) \tag{8}$$

$$\phi_1 = \pi \mu_0 \big(r_1^2 H + r_\mathrm{s}^2 M\big) \tag{9}$$

$$\phi_3 = \pi \mu_0 \big(r_3^2 H + r_\mathrm{s}^2 M\big) \tag{10}$$

$$e_1 = -\pi \mu_0 N_1 \big(r_1^2 \frac{\mathrm{d}H}{\mathrm{d}t} + r_\mathrm{s}^2 \frac{\mathrm{d}M}{\mathrm{d}t}\big) \tag{11}$$

$$e_3 = -\pi \mu_0 N_2 \big(r_3^2 \frac{\mathrm{d}H}{\mathrm{d}t} + r_\mathrm{s}^2 \frac{\mathrm{d}M}{\mathrm{d}t}\big) \tag{12}$$

The difference in induced voltages between Coil-1 and Coil-3 is expressed as the following equation.

$$e_1 - e_3 = -\pi r_\mathrm{s}^2 \mu_0 \big(N_1 - N_3\big) \frac{\mathrm{d}M}{\mathrm{d}t} \tag{13}$$

The induced voltage includes the time differential of the magneitzation M, $\mathrm{d}M/\mathrm{d}t$, so M can be obtained by integrating the induced voltage as

$$M(t) = -\frac{\int \big(e_1(t) - e_3(t)\big)\mathrm{d}t}{\mu_0 \pi r_\mathrm{s}^2 \big(N_1 - N_3\big)} \tag{14}$$

The block diagram of the measurement system is shown in Fig. 7. The sample is inserted into the middle of the detection coil, which is then inserted into the pulse coil. The pulse coil is sufficiently cooled with liquid nitrogen and then the capacitor is charged. Next, a discharge signal is output to discharge the capacitor and generate a pulsed magnetic field. The signal output by the sensor that detects the magnetization characteristics is input to the ADC, which is triggered by the discharge signal. The measured output signal is numerically integrated by a personal computer to obtain the magnetization characteristics of the sample. The ADC is a National Instrument device with a 22-bit resolution, a record length set to 500 kS, and a sampling rate of 1 MS/s.

4 Measured results

We measured the magnetization characteristics of Nd type and Sm type sintered magnets using a high magnetic field. The cylindrical samples were 20 mm long and 10 mm in diameter. The measurements were done on samples that were cut in the easy and hard magnetization direction. To measure the magnetization characteristics in both directions, we applied a 19.4 T magnetic field. Figure 8 shows the $M - H$ curves of Nd type sintered magnet. Figure 9 shows the $M - H$ curves of Sm type sintered magnet. Table 1 shows the measured results of Nd type sintered magnet. Table 2 shows the measured results of Sm type sintered magnet.

As we see from the results presented in Fig. 8 and Fig. 9, the fabricated measurement system can measure the magnetization characteristics of Nd type and Sm type sintered magnets up to the saturation region for both directions. We found the big difference of the coercive force (H_CB) and maximum energy products (BH_max). More than 15% deviation from those presented in the catalog. This difference occurs from the difference in the

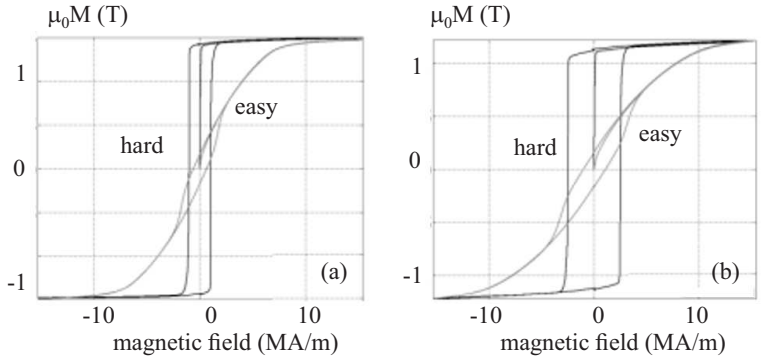

Fig. 8. M-H curves of Nd type sintered magnet: (a) – sample 1, (b) – sample 2

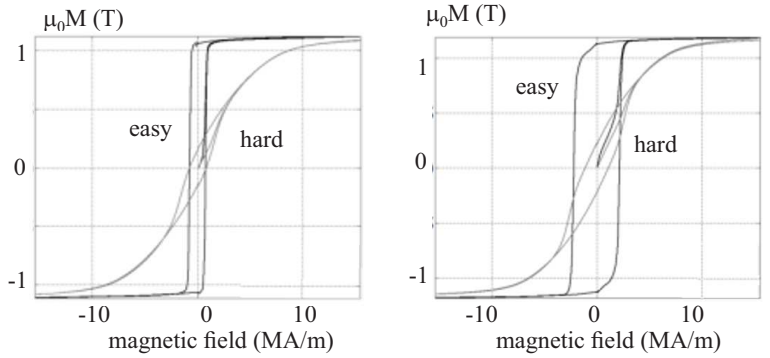

Fig. 9. M-H curves of Smm type sintered magnet: (a) – sample 1, (b) – sample 2

measurement method of effective magnetic field strength (H_{eff}). To measure the effective magnetic field strength, we should decrease the influence of the demagnetizing field and eddy currents as much as possible.

5 Summary

For more accurate measurement of the magnetization characteristics of magnetic materials, we constructed a magnetizer system. The pulsed magnetic field up to 33 T was achieved using fabricated system. Its useful system makes it possible to masure the magnetization characteristics of various magnetic materials in a high magnetic field.

Table 1. Measured results of Nd type sintered magnet

Sample A	Easy	Hard	Catalogue
M_r (T)	1.418	0.168	1.45 –1.51
H_{CB} (kA/m)	866.93	91.07	939 – 1153
H_{CJ} (kA/m)	1024.43	606.50	1.875 –
$BH_{\max}$ (kJ/m^3)	313.87	3.90	405 – 437

Sample B	Easy	Hard	Catalogue
M_r (T)	1.12	0.16	1.10 –1.18
H_{CB} (kA/m)	697.18	92.34	835 – 915
H_{CJ} (kA/m)	2499.27	1051.01	2387 –
$BH_{\max}$ (kJ/m^3)	196.60	3.76	230 – 270

Table 2. Measured results of Sm type sintered magnet

Sample A	Easy	Hard	Catalogue
M_r (T)	1.07	0.16	1.05 –1.12
H_{CB} (kA/m)	579.62	88.90	517 – 796
H_{CJ} (kA/m)	753.30	766.54	557 – 8367
$BH_{\max}$ (kJ/m^3)	174.81	3.48	191 – 239

Sample A	Easy	Hard	Catalogue
M_r (T)	1.12	0.22	1.12 –1.20
H_{CB} (kA/m)	672.85	126.74	780 – 907
H_{CJ} (kA/m)	2174.89	1070.67	1591 – 2387
$BH_{\max}$ (kJ/m^3)	191.12	7.27	223 – 263

References

[1] S. Chikazumi, *Physics of Ferromagnetism* Second Edition, Clarendon Press, Oxford, 1997.

[2] F. Herlach and N. Miura, "High Magnetic Fields, *Science and Technology* vol. 1-3, World Scientific, pp. 2003-2006.

[3] H. Knoepfel, *Pulsed High Magnetic Fields*, North-Holland Publishing Co., 1970.

[4] Y. Nakahata *et al*, "Study of sensor structure for magnetization characteristics measurement high pulsed fields", *J. Jpn. Soc. App. Elec. Mach.* , vol. 19, no. 2, pp. 207-212, (2011).

[5] K. I, Yamada *et al*, "Observation of Barkhausen effect ferromagnetic amorphous ribbon by sensitive pulsed magnetometer", *J. Magnetism and Materials*, vol. 104-107, pp. 341-342, (1992).

Received 13 February 2018